Fundamental research on the role of differential stress in hydraulic fracturing in strength-anisotropic medium

Hayate OHTANI[1], Hitoshi MIKADA[1] and Junichi TAKEKAWA[1]

[1]Dept. of Civil and Earth Res. Eng., Kyoto University

Hydraulic fracturing is a technique to enhance the permeability around the borehole to create fracture networks in oil and natural gas reservoirs. Since the performance of hydraulic fracturing is not fully predictable beforehand, it is important to pre-estimate the extension and the connectivity of artificial fractures for a given condition such as in-situ stress and various mechanical properties of reservoir rock. It, therefore, has been drawing attention to achieve this with a method of numerical simulation in recent years. The propagating direction of hydraulic fractures is the direction of maximum principal stress in an isotropic medium. Since reservoir rock of shale oil or gas is anisotropic in the mechanical properties inferred from several laboratory tests, the propagating direction of hydraulic fractures is strongly affected by the direction of anisotropy axis. Since there are few researches conducted on the numerical simulation of hydraulic fracturing in strongly anisotropic media with the existence of differential stress towards the borehole, it is necessary to examine the role of the differential stress. We give mechanically anisotropic properties such as uniaxial compressive strength, uniaxial tensile strength, permeability, etc., based on the calibration of microscopic parameters of DEM to represent macroscopic parameters of the reservoir rock. The empirical assumption of macroscopic uniaxial tensile strength distribution is introduced into microscopic strength of the model. The result showed that if the differential stress is large, hydraulic fractures tend to propagate in the direction of maximum principal stress whereas hydraulic fractures tend to propagate in the direction of bedding plane under low differential stress. Moreover, this information suggests that in the shale reservoir, which has mechanical anisotropy, the differential stress has important role in estimating the propagation direction of hydraulic fractures.

1. INTRODUCTION

Hydraulic fracturing is an indispensable technique to enhancement of production, and to predict the behavior of hydraulic fractures beforehand is necessary. It is well-known that rocks are heterogeneous and sometimes anisotropic. For example, shale rock is anisotropic in the mechanical properties inferred from uniaxial compression test, Brazilian test, permeability test, etc. In hydraulic fracturing, fractures are likely to propagate in the direction of maximum principal stress, but in anisotropic medium, the propagating direction of hydraulic fractures could be influenced by its aperture plane. Among hydraulic fracturing simulations using distinct element method (DEM), there are some researches in fluid viscosity[1)] and size of particles[1)], pre-existing fractures[2)], and heterogeneity of rock[3)]. On the other hand, there are few researches in the hydraulic fracturing simulation in anisotropic medium. Since failure typically occur along the bedding planes, mechanical anisotropy of reservoir rock could affect the propagating direction of hydraulic fractures. In this research, we calibrate some parameters in DEM to give anisotropy to hydraulic fracturing model first, and then we demonstrated hydraulic fracturing simulations under various differential stress conditions.

2. METHOD

(1) Distinct Element Method

DEM is the method in which a target object is represented as an assembly of circular or spherical particles, and there are imaginary normal and shear springs or bonds between each particle set. Normal and shear forces and moment from springs or bonds act on each particle, and following the behavior of particles enables to simulation of the whole continuum. Our research is two-dimensional simulation, so each particle is assumed to be a circle. Details of 'A bonded-particle model' [4)] can be found in the literature.

(2) Introducing Anisotropy

Kosugi and Kobayashi[5)] conducted the laboratory tests in order to survey the influences of confining

stresses, the inclination of borehole, and pre-existing fractures in hydraulic fracturing. In analyzing results, they proposed the following empirical equation about the tensile strength T_α of rocks with anisotropy.

$$T_\alpha = T_{max}cos^2\alpha + T_{min}sin^2\alpha \quad (1)$$

T_{max} and T_{min} are the maximum and the minimum values of the tensile strength, respectively. 'α=0' means that bedding plane is parallel to the tensile axis, and 'α=90' means that bedding plane is perpendicular to the tensile axis. The tensile axis is the same axis as y-axis in Figure 1. In our research, bedding plane is supposed to correspond with the weak plane.

We applied the macroscopic empirical relation in strength to microscopic parameters as below in our DEM code. Bond's tensile strength $\overline{\sigma_{\theta,\phi}}$ is given as

$$\overline{\sigma_{\theta,\phi}} = \overline{\sigma_{max}}cos^2(\phi-\theta) + \overline{\sigma_{min}}sin^2(\phi-\theta) \quad (2)$$

where $\overline{\sigma_{max}}$ and $\overline{\sigma_{min}}$ are the maximum and the minimum values of bond's tensile strength, respectively. ϕ is the bond's angle, and θ is the anisotropy angle shown in Figure 1.
Similarly, bond's shear strength is given as

$$\overline{\tau_{\theta,\phi}} = \overline{\tau_{max}}cos^2(\phi-\theta) + \overline{\tau_{min}}sin^2(\phi-\theta) \quad (3)$$

where $\overline{\tau_{max}}$ and $\overline{\tau_{min}}$ are the maximum and the minimum values of bond's shear strength, respectively. When bond's angle corresponds with the anisotropy angle, strength of the bond is the maximum.

In order to represent macroscopic permeability, we gave anisotropy to the microscopic parameter; initial aperture $\overline{w_{\theta,\phi}}$ by reference to the equation (1) on the assumption that the anisotropy in permeability might have some relationship with the anisotropy in strength. $\overline{w_{\theta,\phi}}$ is given as

$$\overline{w_{\theta,\phi}} = \overline{w_{min}}cos^2(\phi-\theta) + \overline{w_{max}}sin^2(\phi-\theta) \quad (4)$$

where $\overline{w_{max}}$ and $\overline{w_{min}}$ are the maximum and the minimum values of initial aperture respectively.

There is another factor which is related to the macroscopic anisotropy; bond's Young modulus $\overline{E_{\theta,\phi}}$. Young modulus of the whole continuum E_θ can be obtained by the compliance matrix, and described as the following equation.

$$E_\theta = \frac{E_0E_{90}}{E_0sin^2\theta + E_{90}cos^2\theta} \quad (5)$$

E_0 is the Young modulus obtained when bedding plane is perpendicular to the loading axis (when θ=0), and E_{90} is the Young modulus obtained when bedding plane is parallel to the loading axis (when θ=90). The loading axis is the same axis as y-axis in Figure 1. This macroscopic relation is applied to the microscopic parameter $\overline{E_{\theta,\phi}}$, and described as

$$\overline{E_{\theta,\phi}} = \overline{E_{min}E_{max}} \times [\overline{E_{max}}sin^2(\phi-\theta) + \overline{E_{min}}cos^2(\phi-\theta)]^{-1} \quad (6)$$

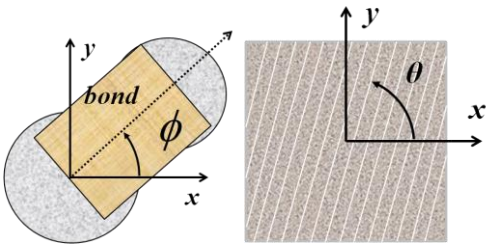

Figure 1 The definition of ϕ and θ

(3) Calibration

Calibrated parameters are shown in Table 1. In calibration, ten realizations are used since the arrangement of particles may have an influence on results. k_s and k_n are the shear and normal stiffness respectively.

Table 1 Calibrated parameters

$\overline{\sigma_{max}}$ [MPa]	27.0
$\overline{\sigma_{min}}$ [MPa]	11.0
$\overline{\tau_{max}}$ [MPa]	180.0
$\overline{\tau_{min}}$ [MPa]	25.0
$\overline{w_{max}}$ [m]	2.0×10^{-6}
$\overline{w_{min}}$ [m]	7.8×10^{-7}
$\overline{E_{max}}$ [GPa]	55.0
$\overline{E_{min}}$ [GPa]	15.0
k_s/k_n	0.43

Target values are referred to the laboratory tests[6), 7)].

These values are UCS (uniaxial compressive strength), BTS (Brazilian tensile strength), and Permeability, and presented in Figure 2, Figure 3, and Table 2. “Orthogonal” in Table 2 means the flow direction is orthogonal to the bedding plane, and “parallel” means the flow direction is parallel to the bedding plane. The results of uniaxial compression test (UCS and Young modulus), uniaxial tensile test (UTS: uniaxial tensile strength), and permeability test (Permeability) are shown in Figures 4 ~ 7. Black dots are average values, and red bars in Figure 2~6 are the ranges of values from the minimum to the maximum. In permeability test, the direction of fluid flow is vertical, and only one model was used since it took a lot of time to demonstrate one permeability test.

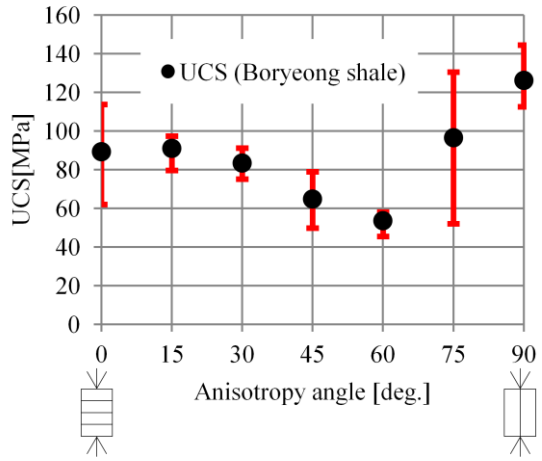

Figure 2 UCS (Cho et al,2012[6])

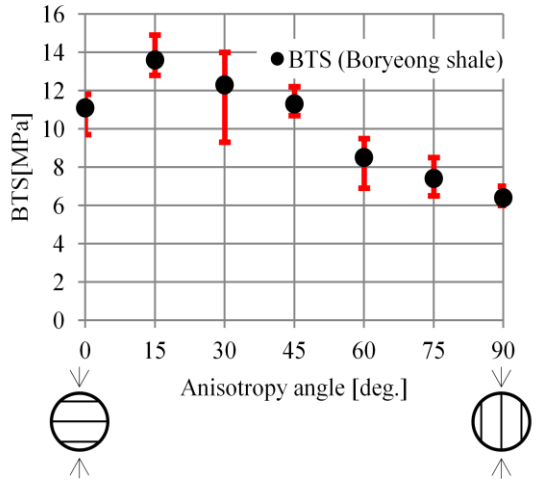

Figure 3 BTS (Cho et al,2012[6])

Table 2 Permeability (Pan et al,2015[7])

	orthogonal	parallel
Permeability [nD]	8.0	199.3 201.3

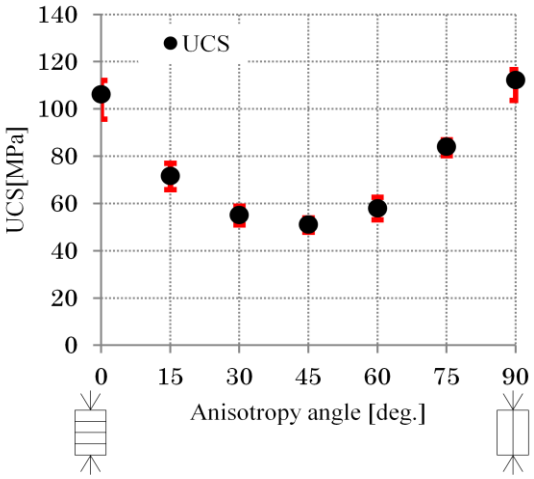

Figure 4 UCS (simulation result)

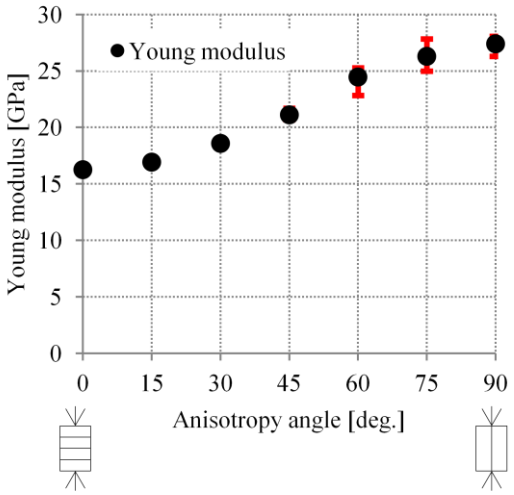

Figure 5 Young modulus (simulation result)

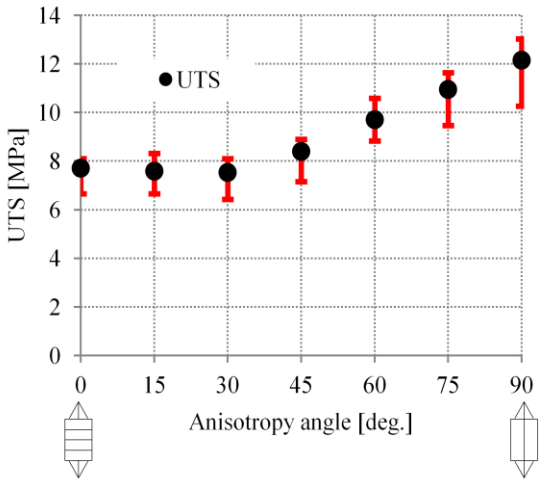

Figure 6 UTS (simulation result)

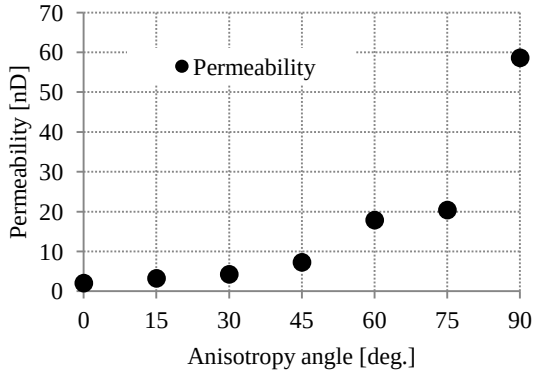

Figure 7 Permeability (simulation result)

(4) Model Settings

This research focuses on hydraulic fracturing in horizontally drilled borehole, and about 400m in depth. Therefore, the bedding plane is supposed to be parallel to the ground surface. The size of the model for hydraulic fracturing simulations is 1.2m in both width and height, and a borehole whose diameter is 0.1m is drilled at the center of the model. There is a wall at each edge of the model. The walls at the left side and under the model are fixed, while the other walls aren't fixed. The non-fixed walls can move depend on the pressure act on each wall, and thereby in-situ stresses can be kept stable. Table 3 shows further conditions in hydraulic fracturing simulation. Hydraulic simulations are demonstrated on different differential stresses shown in Table 4. Vertical direction is defined 'z-direction', and horizontal direction 'x-direction'. The simulation was terminated when hydraulically induced fractures reached the walls or when calculation diverged. In Figure 9, particles are colored yellow, and the bonds which are strong black. As the colors change to white, the bonds become weak. By doing this, bedding planes are represented.

Table 3 simulation conditions

Degree of initial saturation of each pore [%]	0.0
Porosity of the model [%]	4.0
Bulk modulus of fluid [GPa]	2.0
Viscosity of fluid [Pa・m]	0.1×10^{-3}
Flow rate [m^2/s]	5.0×10^{-3}

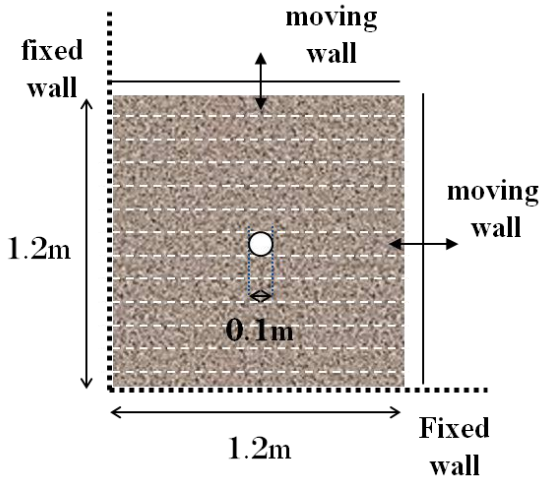

Figure 8 simulation model

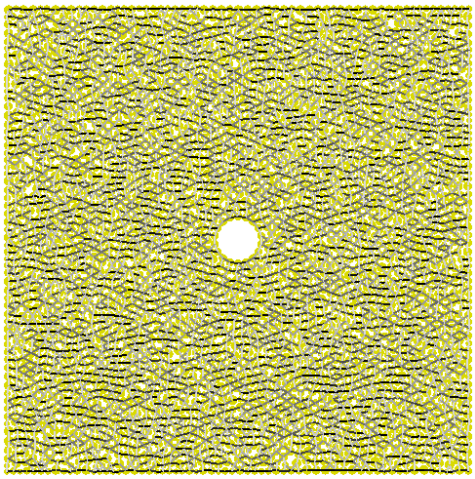

Figure 9 DEM model

Table 4 simulation patterns

	σ_z [MPa]	σ_x [MPa]
Pattern 1 (P-1)	10	5.0
Pattern 2 (P-2)	10	6.3
Pattern 3 (P-3)	10	7.5
Pattern 4 (P-4)	10	8.8
Pattern 5 (P-5)	10	10
Pattern 6 (P-6)	10	12

3. RESULTS AND DISCUSSION

The results of the simulations are presented in Figure 10. The broken bonds which mean generated cracks are expressed as black or red bars. Black bars mean tensile failure had occurred, and red ones shear failures. Saturated pores or unsaturated pores include some fluid are expressed as blue or cyan domains, while pores which don't include fluid are not colored.

Though in hydraulic fracturing simulations using DEM, the results could be influenced by the arrangement of particles to some extent, the propagating direction of hydraulically induced fractures is assumed to be the direction of maximum principal stress in an isotropic medium. The results show that the behavior of hydraulically induced fractures can greatly change as the differential stress is getting smaller. In Figure 10 (a) and (b), there aren't any blanches, and the propagating direction is almost in the direction of maximum principal stress. In Figure 10 (c) and (d), there are some blanches, and the propagating directions are not only in the direction of maximum principal stress but also in the direction of the bedding plane. The results of P-5 and P-6 are in harmony with expectations; the propagating directions are in the direction of the bedding plane

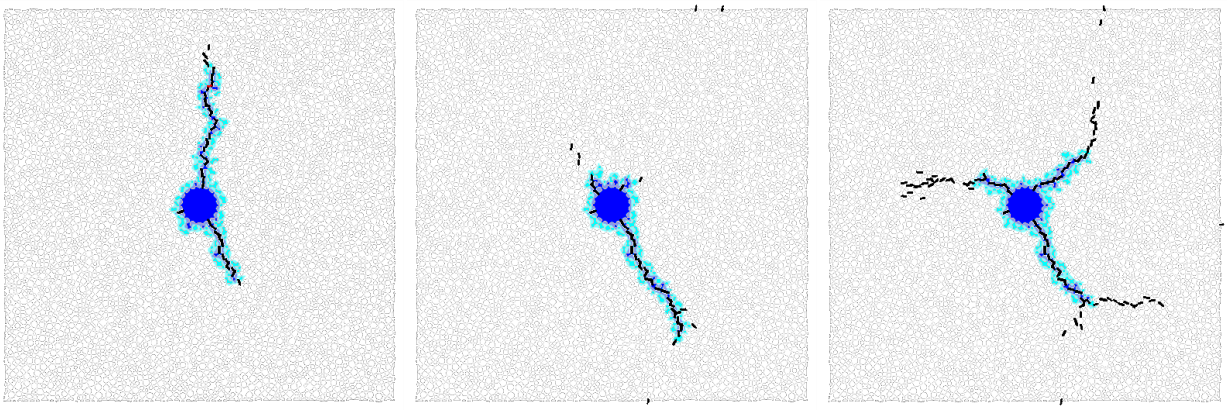

(a) ($\boldsymbol{\sigma_z}$, $\boldsymbol{\sigma_x}$)=(10[MPa],5[MPa]) (b) ($\boldsymbol{\sigma_z}$, $\boldsymbol{\sigma_x}$)=(10[MPa],6.3[MPa]) (c) ($\boldsymbol{\sigma_z}$, $\boldsymbol{\sigma_x}$)=(10[MPa],7.5[MPa])

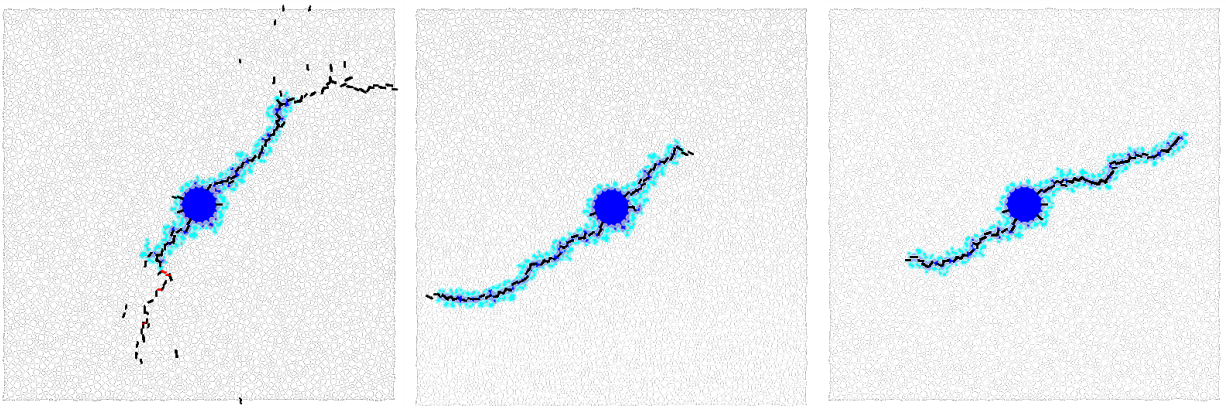

(d) ($\boldsymbol{\sigma_z}$, $\boldsymbol{\sigma_x}$)=(10[MPa],8.8[MPa]) (e) ($\boldsymbol{\sigma_z}$, $\boldsymbol{\sigma_x}$)=(10[MPa],10[MPa]) (f) ($\boldsymbol{\sigma_z}$, $\boldsymbol{\sigma_x}$)=(10[MPa],12[MPa])

Figure 10 Simulation results

as shown in Figure 10 (e) and (f). When the differential stress is comparatively small as in P-3(2.5 [MPa]) or P-4 (1.2 [MPa]), the behavior of fractures is affected by anisotropy in the model and becomes complicated. In P-6, the differential stress is small (2.0 [MPa]), but the direction of maximum principal stress corresponds with the direction of the bedding plane, and the fractures propagated in the direction of maximum principal stress.

4. CONCLUSION

We demonstrated several hydraulic fracturing simulations in an anisotropic media in order to survey the role of differential stress in hydraulic fracturing in strength-anisotropic medium. The results gave us the following information. When differential stress is relatively large like P-1 (5.0[MPa]) and P-2 (3.7 [MPa]), fractures are likely to propagate in the direction of maximum principal stress. However, when differential stress is relatively small like P-3 (2.5[MPa]) and P-4 (1.2 [MPa]), the behaviors are drastically influenced by anisotropy, and complicated fractures are created. When the differential stress is 0.0[MPa], fractures propagate almost along the bedding plane. Even if the differential stress is relatively small, the hydraulically induced fractures will propagate in the direction of maximum principal stress when the direction of maximum principal stress corresponds with the bedding plane.

These results suggest that in the shale rock with strength anisotropy, the differential stress plays an important role in estimating the behavior of hydraulically induced fractures, and anisotropy can be one of the significant factors.

REFERNCES

1) Shimizu, H., Murata, S., and Ishida, T., 2011, The distinct element analysis for hydraulic fracturing in hard rock considering fluid viscosity and particle size distribution, *International Journal of Rock Mechanics & Mining Sciences*, **48**, 712-727

2) Nagaso, M., Mikada, H., and Takekawa, J., 2015, The role of fluid viscosity in hydraulic fracturing in naturally fractured rock, SEG Technical Program Expanded Abstracts, 3214-3218

3) Nagaso, M., Mikada, H., and Takekawa, J., 2016, Mechanism of complex fracture creation on hydraulic fracturing, The 20th International Symposium on Recent Advances in Exploration Geophysics, Extended abstract

4) Potyondy, D.O., and Cundall, P.A., 2004, A bonded-particle model for rock, *International Journal of Rock Mechanics & Mining Sciences*, **41**, 1329-1364

5) Kosugi, M., and Kobayashi H.,1986, *Suiatsuhasaikikou ni okeru ouryokujoutai, kousei no keisha oyobi kizonkiretsu no eikyo –ihouseiganseki ni okeru suiatsuhasai ni kansuru zikkentekikenkyu (dai2hou)-*, *JOURNAL OF THE MINING AND METALLURGICAL INSTITUTE OF JAPAN*, **102**, 567-573

6) Cho, J., Kim, H., Jeon, S., and Min, K., 2012, Deformation and strength anisotropy of Asan gneiss, Boryeong shale, and Yeoncheon schist, *International Journal of Rock Mechanics & Mining Sciences*, **50**, 158-169

7) Pan, Z., Ma, Y., Connell, L.D., Down, D.I., and Camilleri, M., 2015, Measuring anisotropic permeability using a cubic shale sample in a triaxial cell, *Journal of Natural Gas Science and Engineering*, **26**, 336-344